3-2020

Dynamic Magma Storage at Near-Ridge Hot Spots: Evidence from New Galápagos Gravity Data

Z. Cleary
Colgate University

D. M. Schwartz
Boise State University

E. Mittelstaedt
University of Idaho

K. Harpp
Colgate University

This document was originally published in *Geochemistry, Geophysics, Geosystems* by Wiley on behalf of the American Geophysical Union:
Cleary, Z., Schwartz, D.M., Mittelstaedt, E. & Harpp, K. (2020). Dynamic Magma Storage at Near-Ridge Hot Spots: Evidence from New Galápagos Gravity Data. *Geochemistry, Geophysics, Geosystems, 21*(3), e2019GC088722.
https://doi.org/10.1029/2019GC008722

Geochemistry, Geophysics, Geosystems

RESEARCH ARTICLE
10.1029/2019GC008722

Dynamic Magma Storage at Near-Ridge Hot Spots: Evidence From New Galápagos Gravity Data

Z. Cleary[1], D. M. Schwartz[2], E. Mittelstaedt[3], and K. Harpp[1]

[1]Department of Geology, Colgate University, Hamilton, NY, USA, [2]Department of Geosciences, Boise State University, Boise, ID, USA, [3]Department of Geological Sciences, University of Idaho, Moscow, ID, USA

Key Points:
- New gravity data on the eastern islands unexpectedly lack Bouguer anomaly highs that are found on the western islands
- Increases in plume-ridge distance influenced Galápagos volcano construction and magma focusing in the period since 1–2 Ma
- Mantle plume-derived ocean island evolution should be considered thoroughly in the context of plume-ridge interaction

Supporting Information:
- Supporting Information S1

Correspondence to:
Z. Cleary,
zcleary@colgate.edu

Citation:
Cleary, Z., Schwartz, D. M., Mittelstaedt, E., & Harpp, K. (2020). Dynamic magma storage at near-ridge hot spots: Evidence from new Galápagos gravity data. *Geochemistry, Geophysics, Geosystems*, *21*, e2019GC008722. https://doi.org/10.1029/2019GC008722

Received 24 SEP 2019
Accepted 21 FEB 2020
Accepted article online 24 FEB 2020

Abstract A morphological dichotomy exists between the active western and older (>1–2.5 Ma) eastern volcanoes of the Galápagos Archipelago. All of the young shield volcanoes in the west have calderas, but none are present on the older volcanoes in the east. This striking difference suggests that there has been a change in volcanic construction and magmatic supply processes, a finding dissimilar to the prevailing Hawaiian model of hot spot evolution. Bouguer anomaly highs (30–50 mGal) consistent with dense cumulate bodies are measured over these calderas. In contrast, we present new gravity data from Santa Cruz and San Cristóbal islands that lack comparable gravity highs. We propose that formation of shallow magma reservoirs and their associated Bouguer anomaly highs were inhibited during evolution of the eastern volcanoes because the proximal Galápagos Spreading Center diverted plume material more efficiently ~1–2 Ma when the spreading center was ~100 km closer to the plume. The difference in caldera expression between the western and eastern islands may be a surface expression of this process. These results suggest that plume-ridge interaction may play a first-order role in the evolution of magmatic plumbing systems of near-ridge ocean islands, which account for one third of hot spot systems.

Plain Language Summary In the Galápagos Archipelago, a striking dichotomy exists in that volcanic islands in the west have calderas, but those in the east do not. In the Galápagos Archipelago, however, we observe dramatically different volcano shapes and lava chemistry between the younger western and older eastern islands. Our study uses new gravity measurements to investigate differences in the magma plumbing between the eastern and western Galápagos volcanoes and how the plumbing has affected the evolution of surface features. Two of the older, more easterly volcanoes, San Cristóbal and Santa Cruz, lack the gravity highs observed on the western volcanoes, indicating that neither island developed a shallow, dense magma chamber. We propose that this shift in the magmatic system was driven by an increase in the distance between the mantle plume and the nearby mid-ocean ridge by ~100 km at ~1–2 Ma, which led to higher magma supply to the younger western volcanoes. The difference in caldera expression between the western and eastern islands may be a surface expression of this process. Our findings suggest that plume-ridge interaction may play a critical role in the construction of near-ridge islands, which account for one third of hot spot systems.

1. Introduction

Distinct differences in geometry, vent locations, and structure between volcanoes in the western and eastern parts of the Galápagos Archipelago raise questions about the processes controlling the growth of these ocean islands. In the west, volcanoes have shallow lower and steep upper flanks (e.g., McBirney & Williams, 1969); the eastern volcanoes have shallow slopes from base to summit (e.g., Bow, 1979; Geist et al., 1986). The western volcanoes are dominated by circumferential and radial fissures (e.g., Bagnardi et al., 2013; Bernard et al., 2019; Chadwick & Howard, 1991), whereas faults and fissures tend to be linear on the eastern volcanoes (e.g., Bow, 1979; Schwartz, 2014). Most notably, the younger and active western Galápagos volcanoes up to 1-Ma host calderas ~1–10 km wide and <0.1–1.0 km deep (e.g., McBirney & Williams, 1969), whereas the older, eastern volcanoes (>1–2 Ma; Figure 1; e.g., Bailey, 1976; Bow, 1979; Bow & Geist, 1992; Geist et al., 1986) lack morphological indications of calderas. Though calderas may be obscured during the course of an ocean island's evolution, when compared to other similar emergence age ocean island chains (supporting information Figure S1), the striking absence of calderas from the eastern Galápagos volcanoes raises questions about Galápagos island evolution during transport away from a mantle plume.

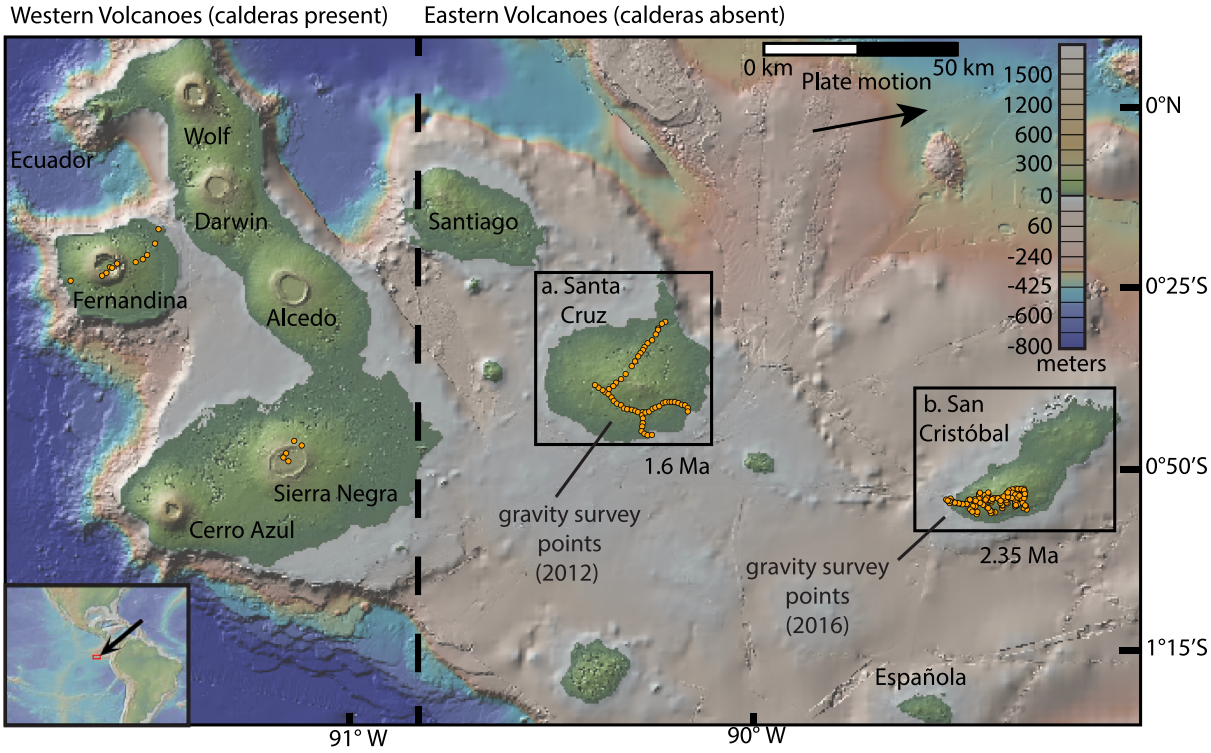

Figure 1. Locations of survey points (orange circles) in this study (a: Santa Cruz and b: San Cristóbal) and previous studies (Fernandina from Case et al., 1973; Sierra Negra from Vigouroux et al., 2008). Approximate shield ages listed for the dormant, eastern volcanoes of the study. Vertical black dashed line separates volcanoes in the caldera-dominated western Galápagos from those in the caldera-free eastern Galápagos. Figure made with GeoMapApp (www.geomapapp.org).

The archetype for the evolution of mantle plume-fed volcanic chains is the Hawaiian Islands. Each Hawaiian island is thought to evolve through morphological and chemical stages correlated to magma supply from the plume (e.g., Morgan, 1971). As seamounts initially form at the periphery of the plume, the low magma flux produces alkalic compositions and small volume lava flows (e.g., Garcia et al., 1993, 1995). Once located above the plume center, volcanoes enter the high magma flux, shield-building stage (e.g., Clague & Dalrymple, 1987; Walker, 1990), often characterized by caldera formation through evacuation of shallow magma chambers, predominantly tholeitic lava compositions, and establishment of relatively dense cumulate cores, which give rise to Bouguer anomaly (BA) gravity highs (e.g., Bagnardi & Amelung, 2012; Flinders et al., 2013; Walker, 1990). After magma flux peaks when the volcano is over the plume center, plate motion carries the island downstream, away from the plume, and magma supply slowly declines toward zero; lava compositions again become predominantly alkalic, and islands begin to subside and erode (e.g., Chen & Frey, 1983; Walker, 1990). Throughout these processes, the island retains the dense cumulate core and therefore the measurable summit gravity high established in the shield-building stage (e.g., Strange et al., 1965).

Many ocean island volcanoes conform to the Hawaiian evolutionary model (e.g., Canary Islands, Carracedo, 1999; Piton de la Fournaise, Albarède et al., 1997), progressing systematically through stages strongly controlled by magma supply and proximity to the plume. Why, then, do volcanoes supplied by the Galápagos plume lack morphological expression of calderas on the older, eastern islands?

One potential explanation for the morphological dichotomy in the Galápagos is that calderas formed during the eastern volcanoes' shield-building stages have since been obscured by surface processes. Erosion of ocean islands strongly depends on annual precipitation rates, which are low in the Galápagos (<2-cm/yr representative precipitation, which corresponds to the spatially averaged mean annual precipitation; Jefferson et al., 2014). Island chains with comparably low precipitation (<2-cm/yr representative precipitation; e.g., Azores, Cape Verde, and Canaries; Jefferson et al., 2014) preserve calderas for up to 4 Ma (Jefferson et al., 2014; Weatherall et al., 2015), making erosion an improbable cause of caldera concealment on the eastern Galápagos Islands (supporting information Figure S1).

Two alternate explanations for the lack of calderas on the eastern Galápagos islands are that infilling by lavas could mask caldera morphology, as suggested on Lord Howe Island (McDougall et al., 1981), Kauai (Macdonald, 1965), and East Molokai (Macdonald, 1965), or that calderas never formed on eastern Galápagos islands. If calderas never formed on the eastern islands, this would provide circumstantial evidence of a change in the islands magmatic systems between east and west. Gravity measurements have the potential to provide more insight into potential differences in the magmatic plumbing systems of the eastern and western volcanoes, as well as how magma supply may control volcanic structure.

In the western Galápagos, previous gravity measurements across the archipelago's younger volcanoes, Fernandina (Case et al., 1973) and Sierra Negra (Vigouroux et al., 2008), reveal 30- to 50-mGal complete BA highs localized over the caldera centers. A positive BA above ocean island volcanoes is commonly interpreted as the expression of cumulate bodies formed during cooling and rising of long-lived, shallow magma reservoirs as the island is being built, constructing a column of cumulates extending up from the base of the crust (Case et al., 1973; Kauahikaua et al., 2000). Cumulates form as dense minerals (e.g., olivine) crystallize and settle out of the melt, instead of being transported to the surface during evacuation of the magma chamber (Kauahikaua et al., 2000).

If the eastern Galápagos volcanoes had similar magma supply processes to that of the western archipelago today, a positive gravity anomaly should be preserved above the eastern volcanoes' centers, even if they previously had calderas (suggestive of magma supply processes) that are now morphologically obscured, such as by volcanism during a "dying stage" as suggested from study of the western volcanoes (Geist et al., 2014). For example, 25- to 120-mGal highs are observed on Hawaiian volcanoes up to ~5 Ma, an interval longer than that separating the youngest western volcanoes from the oldest eastern volcanoes in the Galápagos (Strange et al., 1965; Kinoshita, 1965; Flinders et al., 2013). Conversely, an absence of gravity highs over the eastern Galápagos volcanoes may indicate dissimilar cumulate structures or a lack of concentrated cumulates underlying the islands, implying that there was a fundamental change in constructional processes and magma supply rates to the archipelago after formation of the eastern volcanoes. Such a change could prohibit the formation of calderas in the first place. In this study, we present new gravity measurements from the eastern Galápagos volcanoes of Santa Cruz (Figure 1a) and of San Cristóbal (Figure 1b). We use these data to understand the abrupt absence of calderas in the older, eastern archipelago and what this absence indicates about magma supply dynamics in the Galápagos.

2. Geology of the Galápagos Archipelago

The Galápagos Archipelago lies on the eastward moving (51 km/Myr; Argus et al., 2011) Nazca plate, ~1,000 km west of the Ecuadorian coast and ~200 km south of the Galápagos Spreading Center (GSC). The GSC overlay the Galápagos mantle plume ~5–8 Ma but has since migrated northeastward and formed the ~100-km-long, right-lateral Galápagos Transform Fault (GTF) at 90°50′W, immediately north of the archipelago (Mittelstaedt et al., 2012; Wilson & Hey, 1995). Magnetic data indicate a GSC spreading rate of 53.2 km/Myr east of the GTF and 55.5 km/Myr west of the GTF (Mittelstaedt et al., 2012; Wilson & Hey, 1995). Interaction between the GSC and the mantle plume has been invoked to explain the construction of the small islands and seamounts in the northern Galápagos (e.g., Harpp & Geist, 2002; Harpp et al., 2003, 2014; Mittelstaedt et al., 2005). In contrast, the large shield volcanoes of the main archipelago are thought to have formed primarily by eruption of partial melts from the underlying Galápagos plume, currently centered southwest of Fernandina (e.g., Villagomez et al., 2007, 2014). Best fit models of deformation associated with seismic events in 2005, 2006, 2007, and 2009 on Fernandina indicate that the volcano is underlain by at least two hydraulically connected magma reservoirs at ~1 and ~5 km below sea level (bsl) (Bagnardi & Amelung, 2012).

The shape of the western Galápagos shield volcanoes has been compared to that of an overturned soup bowl, with steep upper slopes of 15° to 34° (compared to 3° to 6° on Mauna Loa) and shallow lower flanks (McBirney & Williams, 1969). This morphology has been attributed to many factors, including construction from pyroclastic material (Banfield et al., 1956), short lava flows emplaced near the summits (Simkin et al., 1973), and erosion (Rowland et al., 1994), though the prevailing theory is related to the pattern of circumferential fissures on the upper flanks and radial fissures on the lower flanks of the volcanoes (Chadwick & Howard, 1991). The circumferential fissures erupt short lava flows that construct the steep

upper flanks (Simkin et al., 1973), whereas the radial fissures extend downslope, depositing longer lava flows to construct the shallower, lower flanks near the coast (Banfield et al., 1956; Chadwick & Howard, 1991). Both the circumferential and radial fissures are believed to be fed by a centralized, shallow magma chamber (e.g., Bagnardi et al., 2013) suggesting that the overturned soup bowl morphology of the western volcanoes is a manifestation of centralized magma storage and eruption.

In contrast, the shield volcanoes of the eastern Galápagos have gentler slopes that extend all the way to their summits (e.g., Bow, 1979; Bow & Geist, 1992; Geist et al., 1986), distinctly different profiles from those of the western shields (Figure 1). The eastern volcanoes are dominated by swarms of fissures and faults (e.g., Harpp & Geist, 2018; Schwartz, 2014) and satellite seamounts (Schwartz, Soule, et al., 2018) that are predominantly NE oriented and lack any evidence of calderas (Figure 1).

Santa Cruz and San Cristóbal, where the gravity data of this study were collected, are two of the largest islands of the eastern archipelago. San Cristóbal consists of two shield volcanoes constructed between 2.35 Ma and several hundred thousand years ago, with a region of young volcanism along the northern coast that was active from ~170 to 5 ka (Bailey, 1976; Geist et al., 1986; Mahr et al., 2016). Santa Cruz's most recent activity is focused in two phases, with island emergence from 1.6 to 1.2 Ma and shield building from 0.7 to 0.1 Ma (Schwartz, 2014). Both islands lack the radial and circumferential fissures of the western islands; instead, the islands host aligned vents, fissures, and faults (Harpp & Geist, 2018; Schwartz, 2014).

3. Gravity Data Collection

Gravity data examined in this study were collected during two surveys, one on the island of Santa Cruz and another on the southwest shield of San Cristóbal. For both surveys, measurements were collected using a Model G LaCoste and Romberg gravimeter sourced from the Potential Fields Equipment Pool facility at Woods Hole Oceanographic Institute (WHOI). In addition to gravity measurements, latitude, longitude, and elevation were collected at each measurement location using a Trimble R7 and R9 GPS for Santa Cruz and San Cristóbal, respectively. For both surveys, the gravimeter's temperature and voltage were also monitored throughout the survey to detect potential anomalies in the data collection. To prevent thermal fluctuations, the gravimeter was connected to a power source two days before the surveys were initiated to achieve thermal stability of the instrument's components. Transport of the gravimeters from WHOI to the survey locations involved a significant change in latitude; thus, a nulling procedure was performed to ensure the instruments' counter readings were in the appropriate range for the latitude of the Galápagos Archipelago. The instrument was hand carried from WHOI to the survey sites and suffered no jarring impacts during transport, which we deemed as conditions that did not warrant further calibration after arriving on site.

3.1. Santa Cruz

In 2012, we conducted a 28-hr gravity survey across Santa Cruz Island. We collected 65 measurements at ~1-km intervals along four survey lines that radiated from a central base station (Figure 2a). All measurements were collected just off the main roadway and include the gravity measurement and latitude, longitude, and elevation collected using a Trimble R7 GPS system. The gravity data are tied to a previous measurement at the Charles Darwin Station dock in Puerto Ayora (Ryland, 1971).

At each survey location, gravity measurements were repeated until at least three values were determined within 0.01 instrument units (~0.01 mGal). The distance and the bearing from the gravimeter to the reference receiver and the height of the reference receiver were measured at every survey location. To account for daily gravimeter drift, a base station was established near the town of Santa Rosa, and measurements were collected every 4 to 6 hr throughout active surveying (Schwartz, 2014). The total drift in base station values over the 28-hr period was ~0.01 mGal.

3.2. San Cristóbal

In 2016, we conducted a 15-day gravity survey across San Cristóbal Island. Following all accessible roads, we collected 179 measurements at ~500-m intervals across the southwestern shield of San Cristóbal (Figure 2b). Measurements were made on either asphalt or hard-packed dirt roads. The gravity data are tied to a previous measurement established by the U.S. Navy on a concrete pier in Baltra, Santa Cruz (0°26′3″S, 90°17′1″W).

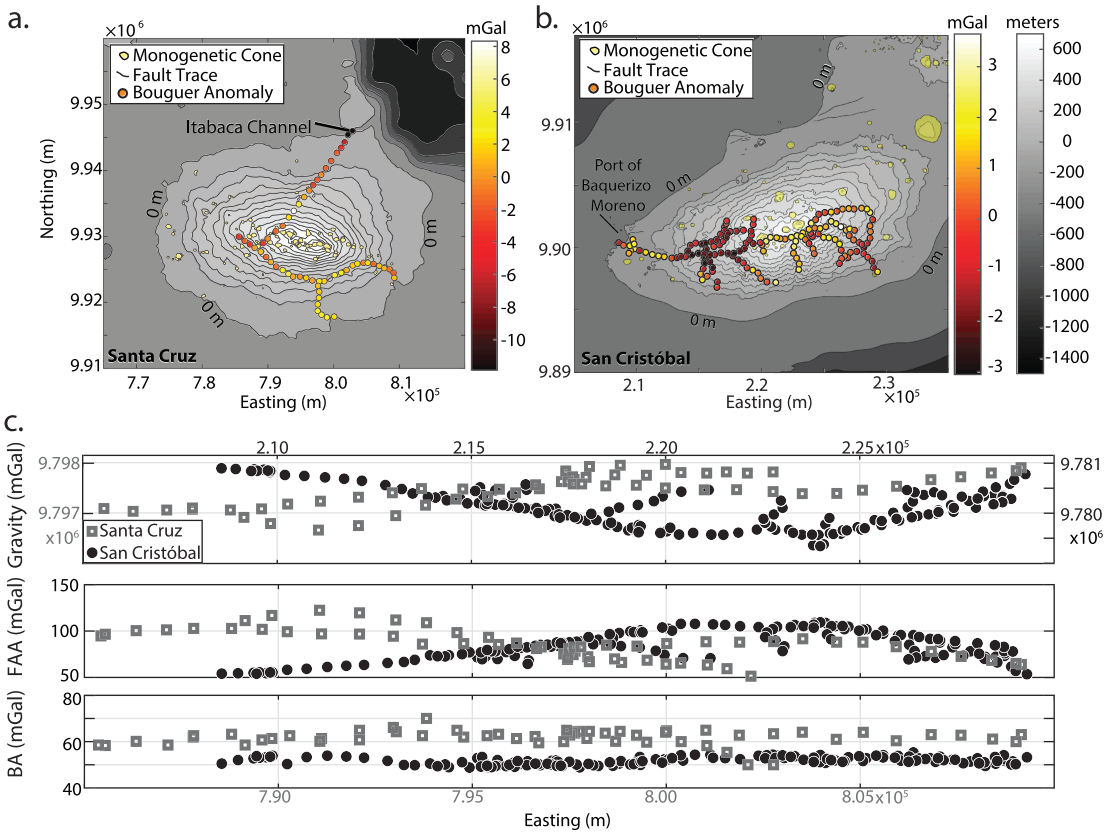

Figure 2. Gravity data from the surveys performed as part of this study were used to calculate the Bouguer anomaly (BA) for (a) Santa Cruz and (b) San Cristóbal. For each island, (c) the (top) measured gravity, (middle) free air anomaly (FAA), and (bottom) Bouguer anomaly (BA) are shown. Note that color differences in Gravity axis labels correspond to the appropriate colors of the data symbols (Santa Cruz, gray and left axis; San Cristóbal, black and right axis).

At each survey location, gravimeter measurements were collected identically to those during the Santa Cruz survey. To account for daily gravimeter drift, two types of base stations were used: (1) daily base stations established to quantify drift throughout a single day and (2) base stations located in Puerto Baquerizo Moreno (PBM), San Cristóbal where measurements were collected every morning and evening to quantify day-to-day drift. Base stations in PBM were maintained for several days, but human activity required changes to our base station location in PBM during the survey period. Ties between the different PBM base station locations were performed to ensure consistency. To constrain instrument drift throughout the survey, we applied a linear fit to all PBM base station data, yielding an average instrument drift of ~0.01 mGal/day.

The instrument was kept at a constant temperature throughout most of the fieldwork period by direct connection to a power source or the use of portable batteries. However, during the San Cristóbal survey, a 2-hr power disruption on 21 July caused the gravimeter to cool from its standard 50.2 to ~44 °C. Once the power loss was noted, a battery was connected and measurements were taken at a PBM base station hourly for 4 hr to quantify the impact of the thermal fluctuations. Measurements indicated a maximum difference of 0.7 mGal from previous base station measurements. This difference decreased until reaching a steady value of 0.2 mGal 4 hr after the initial power loss. We assigned this offset as the new thermal equilibrium of the components and accounted for this shift in our drift calculations.

4. Gravity Anomalies and Modeling

Raw gravity measurements are reduced to a free air anomaly by removing instrument drift (~0.01 mGal/day), the effect of elevation above sea level, and the WGS-84 reference ellipsoid. We calculate the BA by removing the effect of subaerial masses using average densities for Santa Cruz (2,300 kg/m^3) and

San Cristóbal (2,275 kg/m^3) that minimize correlation of the BA with elevation and by adding the gravitational effect of the mass deficits of the surrounding ocean basins (assuming an ocean density of 1,050 kg/m^3; supporting information Figure S3). To determine the average density for the BA correction for Santa Cruz and San Cristóbal volcanoes, we tested effective island densities between 2,000 and 2,600 kg/m^3 at 25-kg/m^3 intervals and chose the value that minimized the correlation of the BA with elevation. The gravitational effect of subaerial masses and the surrounding bathymetry are calculated using a grid of rectangular prisms measuring 30 × 30 m and 61 × 61 m in the *x*-*y* plane on Santa Cruz and San Cristóbal, respectively (equal to the resolution of the corresponding topographic grids; d'Ozouville et al., 2008 for Santa Cruz and GeoMappApp for San Cristóbal). To facilitate examination of relative differences in gravity, the mean anomaly value for each island is removed from the BA. For the remainder of the text, BA values are presented as deviations from the mean.

For this study, we restrict our examination to the complete BA and do not remove the gravitational effect of flexure as done in other locations such as Hawaii (Flinders et al., 2010, 2013). The flexure correction in the Galápagos does not emphasize local gravity anomaly features on a single island. Unlike Hawaii where islands act as isolated loads on the plate, the Galápagos Archipelago is built atop an ~3,000-m-thick volcanic platform that spans the islands and acts as the primary flexural load (e.g., Feighner & Richards, 1994; Karnauskas et al., 2017) leading to a long-wavelength gravitational signal (supporting information Figure S2).

To test for the gravitational signal of cumulate piles similar to those proposed for Fernandina (Case et al., 1973), we calculate the gravitational acceleration at our observation points caused by a vertically oriented, rectangular prism (e.g., Mittelstaedt et al., 2014) with a uniform density contrast of +600 kg/m^3 (estimated density contrast of cumulate pile beneath Fernandina caldera by Case et al., 1973). The calculations are designed to test the effect of cumulate piles caused by small end-member magma chambers. The depth to the bottom of the prism is fixed at 12 km bsl (approximate base of the crust; e.g., Feighner & Richards, 1994) while the depth to the prism top (0–5 km bsl) and the north-south (±10 km) and east-west (−10 to +14 km Santa Cruz; −14 to +10 km San Cristóbal) distance of the prism center from the volcano summit are varied systematically to create a three-dimensional grid of prism locations. Two different prism widths are tested: 2.5 km × 2.5 km and 4.5 km × 4.5 km. The smaller prism corresponds to estimates for active magma chamber widths in the Galápagos (e.g., Fernandina from Bagnardi & Amelung, 2012; and Wolf Volcano from De Novellis et al., 2017), and the larger prism is a conservative estimate of the width of cumulates beneath Galápagos volcanoes, which may reach 25 km laterally (Tepp et al., 2014).

5. Results

5.1. Free Air and Bouguer Anomalies

The free air anomaly has a total range of 70.6 mGal on Santa Cruz and 55.9 mGal on San Cristóbal, both positively correlated with elevation (Figure 2c). Deviations from the mean BA over the southwestern shield of San Cristóbal Island vary between −3.1 and 3.6 mGal and are uncorrelated with elevation (R^2 = 0.0149; Figure 2c). Similarly, deviations from the mean BA on Santa Cruz vary between −9.9 and 7.8 mGal and are uncorrelated with elevation (R^2 = 0.0045; Figure 2c). Relative differences in the BA across each island are mainly short wavelength (<5 km; Figures 2a and 2b).

5.2. Modeled Cumulate Piles

Results of our model prism calculations on San Cristóbal and Santa Cruz are presented as three-dimensional contours of the root-mean-square (RMS) misfit between our observed BA values and values calculated for each horizontal and vertical position of the model prism across the grid of prism locations (Figure 3); smaller misfits indicate a better approximation of the observed gravity anomaly for a particular prism location. On both San Cristóbal and Santa Cruz, the misfit increases with shallowing of the top of the prism (i.e., shallower cumulate pile) and decreasing lateral distances of the prism from the volcano summit. The lack of observations near the summit of Santa Cruz limits quantitative comparison in this area. However, we find significant differences in BA shape between the calculated and observed values for all prism locations on San Cristóbal and Santa Cruz, whether beneath the volcano center or near the coast (Figures 3b, 3d, 3f,

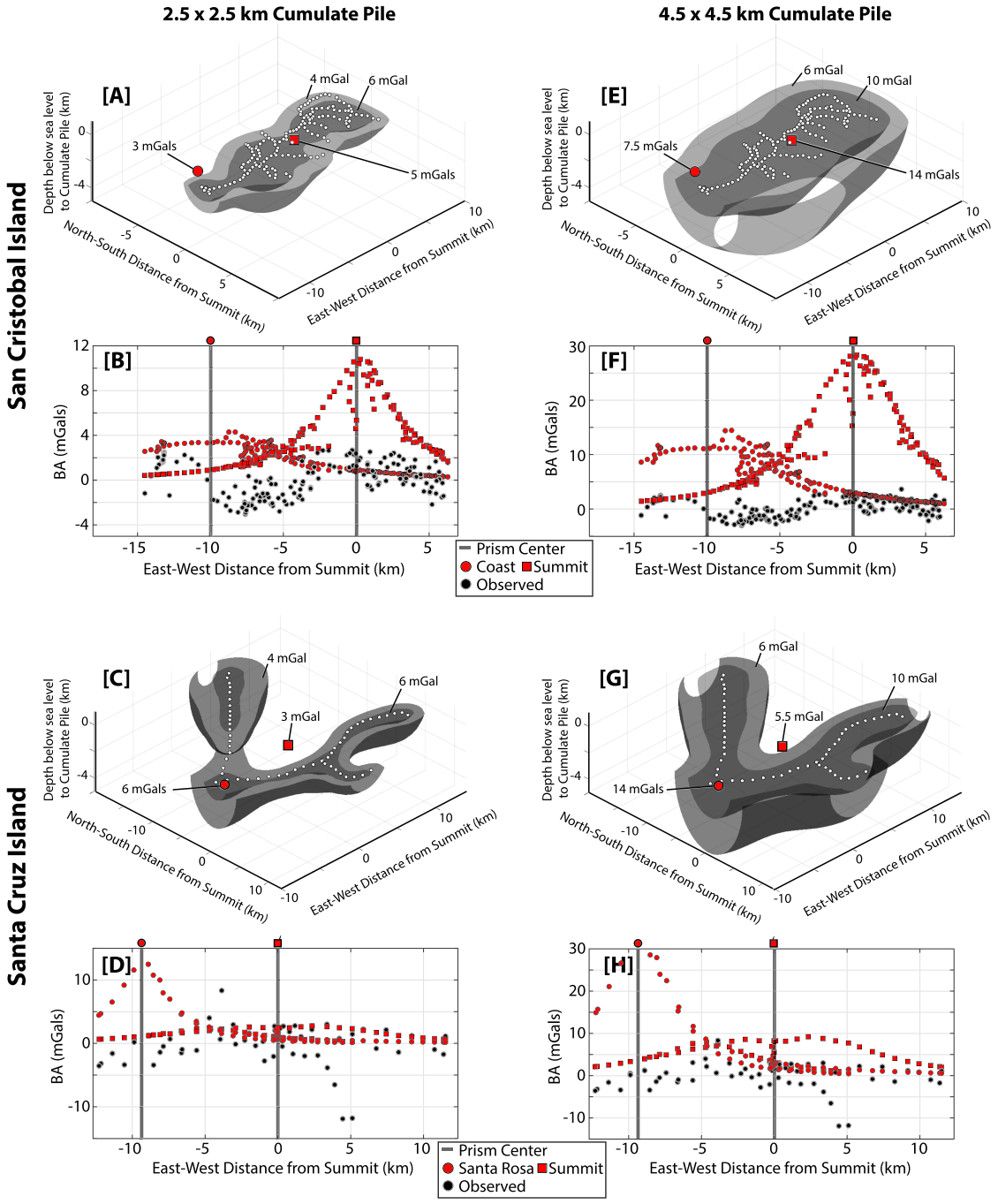

Figure 3. To calculate the effect of a cumulate pile associated with a potential former shallow magma chamber beneath San Cristóbal and Santa Cruz, we calculate the gravitational acceleration due to a single, vertically oriented prism with constant density contrast (+600 kg/m^3) and square lateral extent of (a, b, c, and d) 2.5 km or (e, f, g, and h) 4.5 km. Contours (labeled) of RMS misfit for each prism location between observed gravity (white circles show the location of gravity observations) and the simulated gravity due to cumulate piles show increasing misfit with (a, b, e, and f) decreasing depth to the prism top and decreasing distance from the volcano summit of San Cristóbal and with (c, d, g, and h) decreasing depth to the prism top and distance from the town of Santa Rosa on Santa Cruz. Note that data were not collected near the summit of Santa Cruz. In addition to RMS misfit, we note that (b, d, f, and h) modeled prisms with a depth to their top of 1 km below sea level exhibit anomaly shapes that differ significantly from observed values for both the 2.5- (San Cristóbal) and 4.5-km-wide prism (San Cristóbal and Santa Cruz). The RMS misfit of these profiles are marked by red symbols as indicated in the legends and the symbols above plots in panels (b), (d), (f), and (h). See text for a discussion of prism size.

and 3h). Overall, comparisons between our model and the observations fail to support the presence of large cumulate bodies associated with shallow magma chambers beneath either Santa Cruz or San Cristóbal volcanoes.

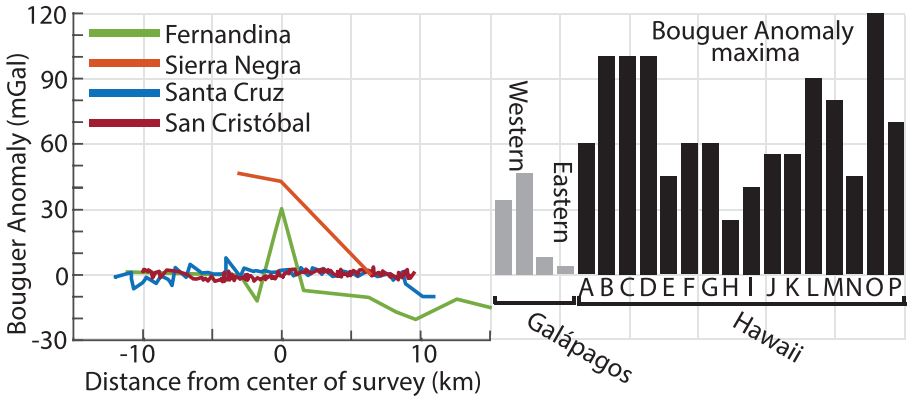

Figure 4. (left) Bouguer anomaly (BA) values for Galápagos volcanoes illustrating differences between the eastern (Santa Cruz and San Cristóbal) and the western volcanoes (Fernandina and Sierra Negra). (right) BA maxima for Galápagos (gray) and residual BA maxima for Hawaiian volcanoes (BA with the flexural component removed; black; A = Kilauea, B = Mauna Loa, C = Mauna Kea, D = Kohala, E = Hualalai, F = Haelekala, G = Kahoolawe, H = West Maui, I = Lanai, J = East Molokai, K = West Molokai, L = Koolau, M = Waianea, N = Kaena, O = Kauai, and P = Niihau; Flinders et al., 2013) highlight the anomalously small maxima over the eastern Galápagos volcanoes.

6. Discussion

If the Galápagos volcanoes follow a pattern of systematic growth and decay, gravity highs arising from the cooling of shallow magma reservoirs similar to those of the western Galápagos are expected to be present in the eastern Galápagos. Correspondingly, the original observation of the striking absence of calderas can support this drastic change in volcano construction. Our finding that the eastern Galápagos volcanoes lack gravity highs implies that systematic volcano growth and decay may not be the most applicable categorization for Galápagos volcano evolution.

6.1. Masking of Caldera Morphology by Lava Infilling

Infilling by late-stage lavas could conceal former calderas. If calderas formed by similar volcanic processes as those in the western volcanoes existed on either Santa Cruz or San Cristóbal and have since been infilled by late-stage lavas, BA highs comparable to the 30- to 50-mGal signals on Fernandina and Sierra Negra should be detectable on the older, eastern volcanoes. Long-lived (~5 Myr) gravity anomaly highs are observable above other extinct volcanic centers covered by younger lavas (Figure 4; i.e., Hawaii; Strange et al., 1965; Kinoshita, 1965; Clague & Dalrymple, 1987; Flinders et al., 2013). The lack of large (>30 mGal) gravity highs (Figures 3 and 4) and the discrepancy between gravity measurements and modeled cumulate columns indicates that no dense cumulate body exists below the surface on Santa Cruz or the southern shield of San Cristóbal. Thus, our results suggest that prior to ~1–2 Ma, major Galápagos volcanoes formed without long-lived shallow magma chambers: at ~1–2 Ma, there was an abrupt change in Galápagos volcano construction mechanisms, which subsequently encouraged formation of large calderas on the young western Galápagos shields (Figures 3 and 4).

6.2. Small, Unfocused Magmatic Systems or Large, Centralized Magma Chambers

The existence of the large calderas across the western Galápagos indicates that this region, located near or over the plume center, is supplied by a high magma flux (e.g., Geist et al., 2014; Poland, 2014). Efficient magma focusing into large, centralized magma chambers has been shown to favor the construction of calderas (Monro & Rowland, 1996). Monro and Rowland (1996) further conclude from the lack of radial rift zones on Galápagos volcanoes (Chadwick & Howard, 1991; Simkin et al., 1973; Nordlie, 1973) that magma storage on the western Galápagos shields is focused into centrally located reservoirs, a finding supported by more recent deformation studies (e.g., Bagnardi & Amelung, 2012; Vigouroux et al., 2008). Consequently, formation of the western shields and their large calderas requires efficient magma focusing and robust magma supplies. Elevated magma supply to the western volcanoes is also consistent with the radial and circumferential fissures that dominate the western volcanoes and control their morphologies; the formation of

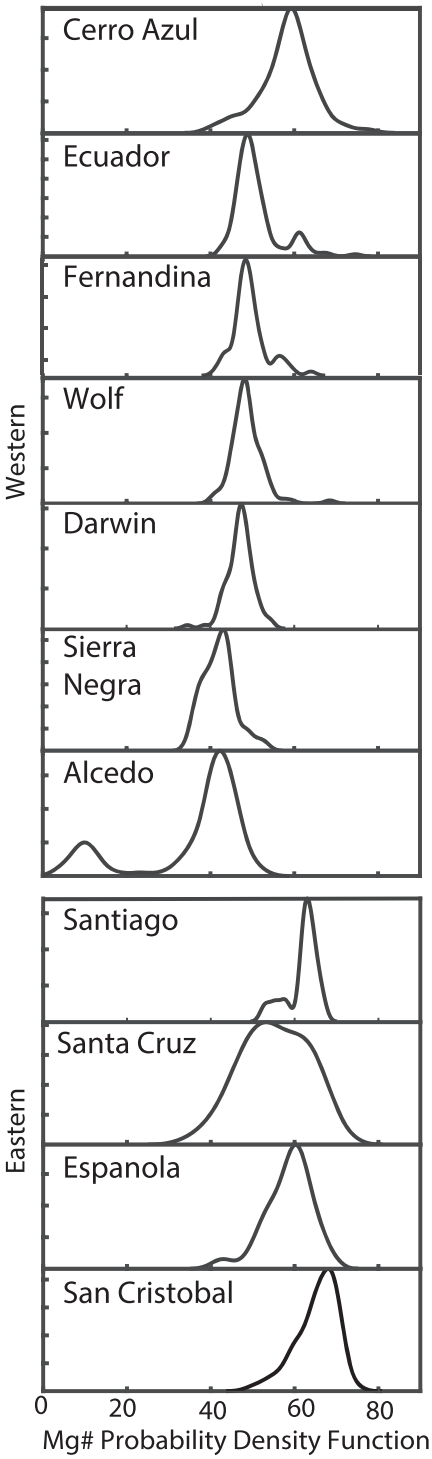

Figure 5. Magnesium number (Mg#) probability density functions for Galápagos volcanoes with median value (MD) and interquartile range (IR). Mg# is defined as Mg/(Mg + Fe). Values for MD and IR of Galápagos volcanoes are Cerro Azul-MD: 58.39, IR: 7.00; Ecuador-MD: 50.88, IR: 4.67; Fernandina-MD: 49.47, IR:3.62; Wolf-MD: 48.72, IR: 3.96; Darwin-MD: 47.05, IR: 3.37; Sierra Negra-MD: 42.11, IR: 4.78; Alcedo-MD: 35.76, IR: 9.24; Santiago-MD: 61.85, IR: 2.51; Santa Cruz-MD: 55.24, IR: 12.80; Espanola-MD: 58.55, IR: 6.83; San Cristóbal-MD: 65.27, IR:6.19). See supporting information Table S1 for bin numbers and references.

these fissures has been attributed to magmatic pressure from underlying diapir-shaped reservoirs (Bagnardi & Amelung, 2012).

Magnesium number (Mg#; [MgO/(MgO + FeO)]) can be interpreted as a measure of magmatic temperature (e.g., Geist et al., 2014) and is, therefore, a useful indication of different magmatic processes. The Mg# of magma decreases with increasing amounts of crystallization; lower Mg# values correspond to cooler, more evolved material. In their mature shield-building stages, western Galápagos volcanoes (e.g., Fernandina) produce lavas with relatively evolved (i.e., low), limited Mg# ranges (Mg# 50.44 ± 4.85 2σ; Figure 5; supporting information Table S1). Geist et al. (2014) suggest that the high magma supply associated with the volcanoes' location near the plume permits development of thermally equilibrated, long-lived, networked sills. Within these thermochemically buffered sills, extended storage periods permit fractionation and homogenization of the magma, resulting in compositionally monotonous lavas with moderately evolved compositions.

By contrast, the eastern Galápagos volcanoes lack rift zones, radial, and circumferential fissures, and, as proposed herein, calderas, indicating a first-order difference in crustal stresses. Instead, the eastern volcanoes exhibit morphologies that are dominated by linear features, faulting, and aligned vent systems (e.g., Bow, 1979; Geist et al., 1986; Harpp & Geist, 2018; Schwartz, 2014); in other words, the morphologies of the eastern volcanoes are inconsistent with the stress fields generated by major magma chambers. Instead, their structures may reflect the regional influence of the then-proximal GSC (e.g., Harpp & Geist, 2002).

Furthermore, eastern Galápagos lavas exhibit greater Mg# variation and more primitive compositions than is observed for the western shield volcanoes (Mg# 59.77 ± 7.60 2σ Figure 5 and Table 1; Harpp & Geist, 2018). Harpp and Geist (2018) attribute the more heterogeneous compositional variations across the eastern archipelago to magma-starved conditions, in which lower magmatic fluxes limit magmatic system development to small, ephemeral, and isolated magma bodies that erupt from distributed vent systems (e.g., Geist et al., 1986; Harpp & Geist, 2018; Schwartz, Wanless, et al., 2018; Wilson, 2013); such magma-starved systems prevent the formation of the long-lived magmatic architecture necessary to support caldera formation (e.g., Monro & Rowland, 1996). An analogous chemical phenomenon is observed at mid-ocean ridges. Mid-ocean ridges with higher spreading rates produce shallow, relatively homogeneous, and more differentiated lavas than slower spreading mid-ocean ridges (Rubin & Sinton, 2007). The characteristic differences between the lavas erupted at fast and slow spreading ridges are consistently explained by the presence or absence of a shallow magma lens (e.g., Sinton & Detrick, 1992). Crucially, the ability to maintain a shallow magma reservoir (i.e., a reservoir capable of producing cumulate mush zones and caldera forming eruptions) is directly related to the thermal buffering afforded by a high magma supply (e.g., Blundy & Annen, 2016; Cashman et al., 2017).

Thus, we propose that since 1–2 Ma, there has been a fundamental change in the intensity of the magma supply and consequently the constructional mechanisms responsible for Galápagos volcanoes (Harpp & Geist, 2018). Prior to 1–2 Ma, when the present-day eastern islands were being built, magma supply was relatively limited. Consequently, magmatic systems

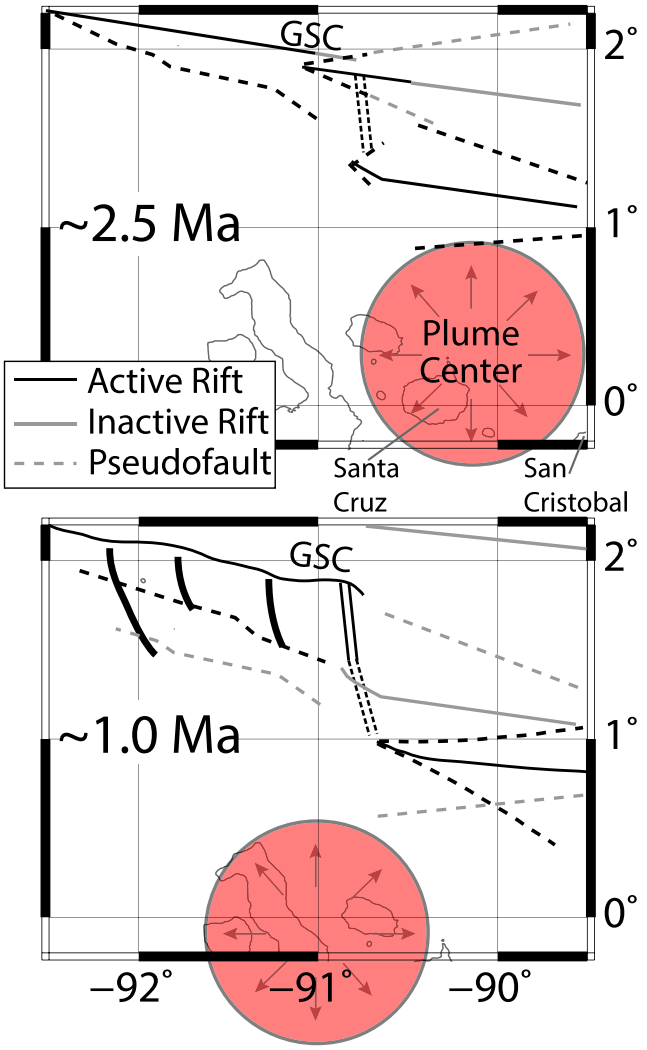

Figure 6. The approximate location of the Galápagos Spreading Center (GSC) and the Galápagos Mantle Plume (shaded circle) at (top) ~2.5 Ma and (bottom) ~1.0 Ma. The island locations are based on the half spreading rate determined by the magnetic modeling of Mittelstaedt et al. (2012). Modified from Mittelstaedt et al. (2012) with permission.

were small, isolated, and short-lived, incapable of supporting the formation of calderas or significant cumulate bodies. Magma had a relatively short residence time in these poorly developed plumbing systems, resulting in widespread compositional heterogeneity across the eastern Galápagos (Harpp & Geist, 2018; Mahr et al., 2016; Pimentel et al., 2016; Wilson, 2013). In contrast, the western Galápagos volcanoes formed with robust magma supplies, sufficient to allow formation of mature, thermochemically buffered magmatic systems, summit calderas, and significant cumulate bodies (Geist et al., 2014).

Our gravity observations support this proposed model, as do recent petrologic studies. Gleeson and Gibson (2019) note that olivines in Santa Cruz lavas, exhibit reverse zonation that reflects multiple recharge and mixing events with primitive peridotitic melts, an observation inconsistent with large, thermally buffered magma systems (e.g., Geist et al., 2014) but plausible in small, poorly networked, ephemeral magmatic systems with low magma supplies (Harpp & Geist, 2018). Furthermore, regional petrologic studies (Geist et al., 1998; Gibson & Geist, 2010) demonstrate that magmas from the eastern and central volcanoes undergo crystallization in the deep and lower crust. This is in contrast to magmas in the western archipelago, which crystallize across a crust-wide mush zone but equilibrate with plagioclase, olivine, and clinopyroxene in the shallow (<3 km) subcaldera magma chambers (Geist et al., 1998; Geist et al., 2014; Stock et al., 2018). The critical advance presented here is that it has never been understood whether the volcanoes of the west evolve into those of the central and eastern archipelago, or if the systematic differences in the depth of fractionation have been maintained over the entire history of the volcano. The new gravity data indicate the latter.

6.3. The Role of Plume-Ridge Interaction in the Galápagos

Chemical and physical observations of plume-affected mid-ocean ridges, as well as analytical and numerical models, indicate that plume material flows toward spreading centers, with the intensity of ridgeward flow increasing as plume-ridge separation decreases (e.g., Detrick et al., 2002; Ito et al., 1997; Ribe, 1996; Schilling et al., 1982; Small, 1995). Prior to 1–2 Ma, plume-ridge distance in the Galápagos was ~100 km less than it is today (Mittelstaedt et al., 2012; Figure 6). Influence of the GSC on plume flow is supported by seismic tomography in the western Galápagos that suggests the plume bends slightly toward the GSC at ~100-km depth and then back toward the main archipelago again ~80-km depth (Villagomez et al., 2014).

The precise mechanism by which plume material is transported to adjacent mid-ocean ridges remains an open question, with two broad categories of competing models: (a) lateral flow away from the plume (e.g., Schilling et al., 1982; Shorttle et al., 2010), guided by the base of the lithosphere (e.g., Bercovici & Lin, 1996) or beneath an anhydrous, high-viscosity mantle layer (e.g., Ito & Bianco, 2014; Kokfelt et al., 2005; Villagomez et al., 2014); and (b) transport of plume material in sublithospheric melt channels toward the ridge (e.g., Morgan, 1978; Schilling et al., 1982; Braun & Sohn, 2003). Recently, Gibson et al. (2015) proposed that when the plume and GSC were superimposed (5–12 Ma; Mittelstaedt et al., 2012; Meschede & Barkhausen, 2000; Wilson & Hey, 1995), the plume stem was "captured" by the ridge, effectively anchoring the plume to the spreading center. As the GSC has migrated northeast since 5 Ma, the plume has remained connected to the ridge via melt transport through a network of channels, resulting in an ongoing supply of enriched, volatile-rich melts that Gibson et al. (2015) have observed along the GSC, NE of the main archipelago, and between the archipelago and the GSC (e.g., Harpp & Geist, 2002). Consequently, even when a ridge

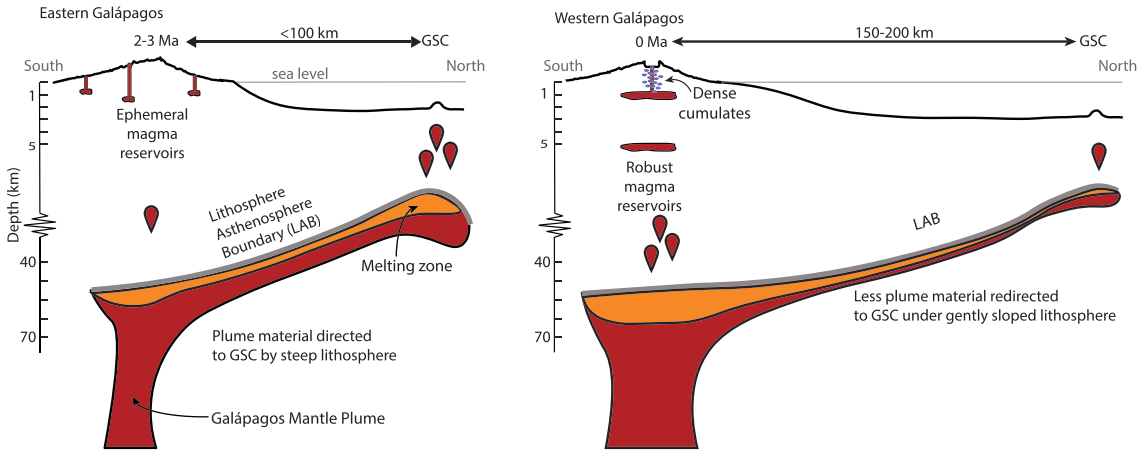

Figure 7. Proposed model for the change in plume supply responsible for the shift in constructional processes over the past 1–2 Ma. Both profiles indicate a south-north profile. (left) "2–3 Ma" represents the eastern Galápagos, where a steep lithosphere enhances buoyant ridgeward plume flow, resulting in a lower magma flux to overlying volcanoes, which are constructed by smaller, ephemeral magmatic systems. (right) "0 Ma" represents the western Galápagos, where a shallow lithosphere (thermal or rheological; e.g., Hall & Kincaid, 2003; Villagomez et al., 2014; thick gray line) diminishes ridgeward plume flow, consequently increasing magma flux to overlying volcanoes and allowing development of shallow magma chambers capable of supporting caldera formation. Estimates of magma sill depths in the western Galápagos volcanoes are 1 and 5 km bsl on Fernandina (Bagnardi & Amelung, 2012) and 2.1–2.3 km bsl on Sierra Negra (Vigouroux et al., 2008). GPS deformation data of Sierra Negra's 2005 eruption indicate a magma sill size of 5.3 km × 3 km (Vigouroux et al., 2008); interferometric synthetic aperture radar data of eruption and seismic events on Fernandina from 2005, 2006, 2007, and 2009 indicate two magma sills with dimensions of 2.8 km × 2.03 km × 1.08 km and 2.7 km × 0.18 km × 4.93 km representing length, width, and depth, respectively (Bagnardi & Amelung, 2012). Lithospheric thickness estimates place the plume stem at depths of 56 to 60 km in the western and 46 to 57 km in the eastern Galápagos (Gibson & Geist, 2010).

is migrating away from a plume, material from the plume continues to be transported toward and incorporated into the magmatic system of the spreading center (e.g., Mittal & Richards, 2017; Gibson & Richards, 2018).

At 1–2 Ma, when the GSC was ~100 km closer to the plume center than it is today, the influence of the ridge on the archipelago would have been considerably greater, with a greater proportion of plume material being diverted toward the GSC axis (e.g., Gibson et al., 2015; Ito & Lin, 1995) than likely occurs today. Consequently, magma supply from the plume to the eastern volcanoes would have been reduced compared to what it is to the present-day western Galápagos shields, thereby preventing development of robust, thermochemically buffered magmatic systems in the 1- to 2-Ma eastern Galápagos Islands. Indeed, a previously greater plume supply to the ridge is consistent with increased gravitationally predicted crustal thicknesses along the GSC before ~1 Ma (Mittelstaedt et al., 2014).

We suggest it is unlikely that the magma-starved characteristics of the 1- to 2.5-Ma eastern Galápagos volcanoes result simply from a reduction in melt supply for the same rate of plume upwelling. The total amount of melting is proportional to melt column length, with longer melt columns generating higher amounts of decompression melting of ascending mantle of uniform composition and temperature (e.g., Langmuir et al., 1992). Furthermore, lithospheric thickness is thought to have a strong control on the depth to the top of the melt column, with thicker lithospheric lids limiting the amount of melting that a parcel of mantle can experience (e.g., Dasgupta et al., 2010; Humphreys & Niu, 2009). To estimate lengths of melt columns responsible for the wide variation in geochemical signatures across the Galápagos, Gibson and Geist (2010) inverted rare earth elements data for lithosphere thickness (e.g., depth to the top of the melting column), and their calculations suggest that lithospheric thicknesses in the western Galápagos are ~56–60 km. By contrast, the lithosphere is ~15 km thinner (on average) in the eastern Galápagos, ranging from 46 to 57 km beneath Santa Cruz, Santiago, and San Cristóbal (Gibson & Geist, 2010). The thinner lithosphere in the eastern Galápagos, therefore, should result in longer melt columns and higher melt supplies to the older volcanoes, which is in direct contrast to geochemical and morphological observations across the archipelago (Figure 5; Harpp & Geist, 2018). Thus, we conclude that the magma-starved characteristics of the eastern Galápagos volcanoes are a manifestation of reduced plume supply related to ridge proximity, not a lower melt flux resulting from lithospheric thickness variations.

6.4. Lithospheric Slope and Plume Supply

Migration of the GTF away from the plume center 1–2 Ma resulted in a ~100-km increase in plume-ridge distance (Mittelstaedt et al., 2012) placing, more gently sloped lithosphere above the plume stem (Figure 7; e.g., Small, 1995) and limiting ridgeward plume flow. Consistently, gravity, magnetic, and bathymetry data predict that there was greater crustal production (Mittelstaedt et al., 2012, 2014) and warmer mantle temperatures (Ito & Lin, 1995) along the GSC at 1–2 Ma than there is today. Gravity inversions by Mittelstaedt et al. (2014) predict ~1- to 3-km-thicker crust on the GSC east of the GTF prior to ~1 Ma, supporting enhanced plume-ridge interaction in the past. Consequently, plume supply to the GSC has likely decreased significantly since 1–2 Ma, resulting in more effective magma focusing beneath the present-day western Galápagos volcanoes and the formation of robust, long-lived magmatic reservoirs supplying caldera-bearing volcanoes (Figure 7).

7. Conclusions

New gravity surveys in the eastern Galápagos reveal that no localized, high-density subsurface body exists beneath Santa Cruz or the southwestern complex of San Cristóbal. The absence of gravity highs in the eastern and central archipelago contrasts with the 30- to 50-mGal gravity highs observed in the western Galápagos and indicates a fundamental change in Galápagos magmatic systems at 1–2 Ma. At 1–2 Ma, the magmatic systems of Galápagos volcanoes underwent a shift from small, diffuse, and ephemeral to robust and highly focused. Prior to 1–2 Ma, the Galápagos plume was closer to the GSC, an arrangement that diverted more plume material to the ridge axis, yielding a lower plume magma flux to the present-day eastern volcanoes. Consequently, the eastern volcanoes were built from small, ephemeral magma chambers unable to support caldera formation. Migration of the GSC away from the plume and lengthening of the GTF through incremental ridge jumps conspired to cause an abrupt increase in plume-ridge separation, reducing ridgeward plume flow and augmenting plume flux to the present-day western islands. This higher plume magma supply promoted construction of large, shallow, long-lived caldera-building magmatic plumbing systems in the western Galápagos.

Currently, the prevailing understanding of ocean island evolution is thought to be controlled primarily by variations in magma supply as volcanoes are transported away from the plume by plate motion; the drastic, sudden change in Galápagos volcano construction conditions contradicts this model. Our study illustrates that changes in plume-ridge distance play a first-order role in the evolution of the Galápagos Archipelago. Consequently, the paradigm of ocean island volcano evolution must be considered more carefully in the context of plume-ridge interaction. Understanding the role of plume-ridge interaction in ocean island evolution is critical given that more than one third of the Earth's hot spots are located within 500 km of spreading centers (Courtillot et al., 2003).

Acknowledgments
This project was funded by National Science Foundation Grants OCE-1347731 and EAR-1145271 and utilized gravimeters loaned from the Potential Fields Equipment Pool facility at the Woods Hole Oceanographic Institution. We are grateful to Hannah Bercovici, Marco Córdova, Jake Mahr, Regina Pimentel, Emily Wilson, Rita Van Kirk, and Purtí for their help with data collection, as well as Captain Lenin Cruz and his ship the Pirata for field support. We extend our gratitude to the Galápagos National Park and the Charles Darwin Research Center for their assistance in studying this beautiful archipelago. Data from this study can be found on the Marine Geoscience Data System (doi: 10.1594/IEDA/326493).

References

Albarède, F., Luais, B., Fitton, G., Semet, M., Kaminski, E., Upton, B. G. J., et al. (1997). The geochemical regimes of Piton de la Fournaise volcano (Réunion) during the last 530,000 years. *Journal of Petrology*, *38*(2), 171–201. https://doi.org/10.1093/petroj/38.2.171

Argus, D., Gordon, R., & DeMets, C. (2011). Geologically current motion of 56 plates relative to the no-net-rotation reference frame. *Geochemistry, Geophysics, Geosystems*, *12*, Q11001. https://doi.org/10.1029/2011GC003751

Bagnardi, M., & Amelung, F. (2012). Space-geodetic evidence for multiple magma reservoirs and subvolcanic lateral intrusions at Fernandina Volcano, Galápagos Islands. *Journal of Geophysical Research*, *117*, B10406. https://doi.org/10.1029/2012JB009465

Bagnardi, M., Amelung, F., & Poland, M. (2013). A new model for the growth of basaltic shields based on deformation of Fernandina volcano, Galápagos Islands. *Earth and Planetary Science Letters*, *377-378*, 358–366. https://doi.org/10.1016/j.epsl.2013.07.016

Bailey, K. (1976). Potassium-argon ages from the Galápagos Islands. *Science*, *192*(4238), 465–467. https://doi.org/10.1126/science.192.4238.465

Banfield, A., Behre, C., & Clair, D. (1956). Geology of Isabela (Albemarle) Island, Archipelago de Colon (Galápagos). *Bulletin of the Geological Society of America*, *67*(2), 215–234. https://doi.org/10.1130/0016-7606(1956)68[215:GOIAIA]2.0.CO;2

Bercovici, D., & Lin, J. (1996). A gravity current model of cooling mantle plume heads with temperature-dependent buoyancy and viscosity. *Journal of Geophysical Research*, *101*(B2), 3291–3309. https://doi.org/10.1029/95JB03538

Bernard, B., Stock, M., Coppola, D., Hidalgo, S., Bagnardi, M., Gibson, S., et al. (2019). Chronology and phenomenology of the 1982 and 2015 Wolk volcano eruptions Galápagos Archipelago. *Journal of Volcanology and Geothermal Research*, *374*, 26–38. https://doi.org/10.1016/j.jvolgeores.2019.02.013

Blundy, J., & Annen, C. (2016). Crustal magmatic systems from the perspective of heat transfer. *Elements*, *12*(2), 115–120. https://doi.org/10.2113/gselements.12.2.115

Bow, C. S. (1979). Geology and petrogenesis of lavas from Floreana and Santa Cruz Islands, Galápagos Archipelago, Ecuador, (Ph.D. thesis): Eugene, University of Oregon.

Bow, C. S., & Geist, D. (1992). Geology and petrology of Floreana island, Galápagos archipelago, Ecuador. *Journal of Volcanology and Geothermal Research*, *52*(1-3), 83–105. https://doi.org/10.1016/0377-0273(92)90134-Y

Braun, M. G., & Sohn, R. A. (2003). Melt migration in plume–ridge systems. *Earth and Planetary Science Letters*, *213*(3-4), 417–430. https://doi.org/10.1016/s0012-821x(03)00279-6

Carracedo, J. C. (1999). Growth, structure, instability and collapse of Canarian volcanoes and comparisons with Hawaiian volcanoes. *Journal of Volcanology and Geothermal Research*, *94*(1-4), 1–19. https://doi.org/10.1016/S0377-0273(99)00095-5

Case, J. E., Ryland, S. L., Simkin, T., & Howard, K. A. (1973). Gravitational evidence for a low-density mass beneath the Galápagos Islands. *Science*, *181*(4104), 1040–1042. https://doi.org/10.1126/science.181.4104.1040

Cashman, K., Stephen, R., & Blundy, J. (2017). Vertically extensive and unstable magmatic systems: A unified view of igneous processes. *Science*, *335*(6331). https://doi.org/10.1126/science.aag3055

Chadwick, W., & Howard, K. (1991). The pattern of circumferential and radial fissures on the volcanoes of Fernandina and Isabela islands, Galápagos. *Bulletin of Volcanology*, *53*, 259–275. https://doi.org/10.1007/BF00414523

Chen, C. Y., & Frey, F. A. (1983). Origin of Hawaiian tholeiite and alkalic basalt. *Nature*, *302*, 785–789. https://doi.org/10.1038/302785a0

Clague, D., & Dalrymple, G. (1987). Hawaiian-Emperor volcanic chain. Part I. Geologic evolution. *Volcanism in Hawaii*, *1*(1350), 5–54. https://doi.org/10.1029/GL002i007p00305

Courtillot, V., Davaille, A., Besse, J., & Stock, J. (2003). Three distinct types of hotspots in the Earth's mantle. *Earth and Planetary Science Letters*, *205*(3-4), 295–308. https://doi.org/10.1016/S0012-821X(02)01048-8

Dasgupta, R., Jackson, M., & Lee, C. (2010). Major element chemistry of ocean island basalts—Conditions of mantle melting and heterogeneity of mantle source. *Earth and Planetary Science Letters*, *289*(3-4), 377–392. https://doi.org/10.1016/j.epsl.2009.11.027

De Novellis, V., Castaldo, R., De Luca, C., Pepe, S., Zinno, I., Casu, F., et al. (2017). Source modelling of the 2015 Wolf volcano (Galápagos) eruption inferred from Sentinel 1-A DInSAR deformation maps and pre-eruption ENVISAT time series. *Journal of Volcanology and Geothermal Research*, *344*, 246–256. https://doi.org/10.1016/j.jvolgeores.2017.05.013

Detrick, R. S., Sinton, J. M., Ito, G., Canales, J. P., Behn, M., Blacic, T., et al. (2002). Correlated geophysical, geochemical, and volcanological manifestations of plume-ridge interaction along the Galápagos Spreading Center. *Geochemistry, Geophysics, Geosystems*, *3*(10), 8501. https://doi.org/10.1029/2002GC000350

d'Ozouville, N., Deffontaines, B., Benveniste, J., Violette, S., & Marsily, G. (2008). DEM generation using ASAR (ENVISAT) for addressing the lack of freshwater ecosystems management, Santa Cruz Island, Galápagos. *Remote Sensing of Environment*, *112*, 4131–4147. https://doi.org/10.1016/j.rse.2008.02.017

Feighner, M., & Richards, M. (1994). Lithospheric structure and compensation mechanisms of the Galápagos Archipelago. *Journal of Geophysical Research*, *99*(B4), 6711–6729. https://doi.org/10.1029/93JB03360

Flinders, A. F., Ito, G., & Garcia, M. O. (2010). Gravity anomalies of the Northern Hawaiian Islands: Implications on the shield evolutions of Kauai and Niihau. *Journal of Geophysical Research*, *115*, B08412. https://doi.org/10.1029/2009JB006877

Flinders, A. F., Ito, G., Garcia, M. O., Sinton, J. M., Kauahikaua, J., & Taylor, B. (2013). Intrusive dike complexes, cumulate cores, and the extrusive growth of Hawaiian volcanoes. *Geophysical Research Letters*, *40*, 3367–3373. https://doi.org/10.1002/grl.50633

Garcia, M. O., Foss, D. J. P., West, H. B., & Mahoney, J. J. (1995). Geochemical and isotopic evolution of Loihi volcano, Hawaii. *Journal of Petrology*, *36*(6), 1647–1674. https://doi.org/10.1093/petrology/37.3.729

Garcia, M. O., Jorgenson, B. A., Mahoney, J. J., Ito, E., & Irving, A. (1993). An evaluation of temporal geochemical evolution of Loihi summit lavas: Results from Alvin submersible dives. *Journal of Geophysical Research*, *98*(B1), 537–550. https://doi.org/10.1029/92JB01707

Geist, D., Bergantz, G., & Chadwick, W. (2014). Galápagos magma chambers. In K. Harpp, E. Mittelstaedt, N. d'Ozouville, & D. Graham (Eds.), *The Galápagos: A natural laboratory for the Earth sciences* (Vol. 1, pp. 55–69). Washington, DC: American Geophysical Union.

Geist, D., McBirney, A., & Duncan, R. (1986). Geology and petrogenesis of lavas from San Cristóbal Island, Galápagos Archipelago. *GSA Bulletin*, *97*(5), 555–566. https://doi.org/10.1130/0016-7606(1986)97<555:GAPOLF>2.0.CO;2

Geist, D., Naumann, T., & Larson, P. (1998). Evolution of Galapagos magmas: Mantle and Crustal Fractionation without assimilation. *Journal of Petrology*, *39*(5), 953–971. https://doi.org/10.1093/petroj/39.5.953

Gibson, S., & Geist, D. (2010). Geochemical and geophysical estimates of lithospheric thickness variation beneath Galápagos. *Earth and Planetary Science Letters*, *300*, 275–286. https://doi.org/10.1016/j.epsl.2010.10.002

Gibson, S., Geist, D., & Richards, M. (2015). Mantle plume capture, anchoring, and outflow during the Galapgos plume-ridge interaction. *Geochemistry, Geophysics, Geosystems*, *16*, 1634–1655. https://doi.org/10.1002/2015GC005723

Gibson, S. A., & Richards, M. A. (2018). Delivery of deep-sourced, volatile-rich plume material to the global ridge system. *Earth and Planetary Science Letters*, *499*, 205–218. https://doi.org/10.1016/j.epsl.2018.07.028

Gleeson, M., & Gibson, S. (2019). Crustal controls on apparent mantle pyroxenite signals in ocean-island basalts. *Geology*, *47*(4), 321–324. https://doi.org/10.1130/G45759.1

Hall, P., & Kincaid, C. (2003). Melting, dehydration, and the dynamics of off-axis plume-ridge interaction. *Geochemistry, Geophysics, Geosystems*, *4*(9), 8510. https://doi.org/10.1029/2003GC000567

Harpp, K., Fornari, D., Geist, D., & Kurz, M. (2003). Genovesa Submarine Ridge: A manifestation of plume-ridge interaction in the northern Galápagos Islands. *Geochemistry, Geophysics, Geosystems*, *4*(9), 8511. https://doi.org/10.1029/2003GC000532

Harpp, K., & Geist, D. (2002). Wolf-Darwin Lineament and plume-ridge interaction in the northern Galápagos. *Geochemistry, Geophysics, Geosystems*, *3*(11), 8504. https://doi.org/10.1029/2002GC000370

Harpp, K., & Geist, D. (2018). The evolution of Galápagos volcanoes: An alternative perspective. *Frontiers in Earth Science Volcanology*, *6*. https://doi.org/10.3389/feart.2018.00050

Harpp, K., Wirth, K., Teasdale, R., Blair, S., Reed, L., Barr, J., et al. (2014). Plume-ridge interactions in the Galápagos: Perspectives from Wolf, Darwin, and Genovesa Islands. In K. Harpp, E. Mittelstaedt, N. d'Ozouville, & D. Graham (Eds.), *The Galápagos: A Natural Laboratory for the Earth Sciences* (Vol. *1*, pp. 285–334). Washington, DC: American Geophysical Union.

Humphreys, E., & Niu, Y. (2009). On the composition of ocean island basalts (OIB): The effects of lithospheric thickness variation and mantle metasomatism. *Lithos*, *112*(1-2), 118–136. https://doi.org/10.1016/j.lithos.2009.04.038

Ito, G., & Bianco, T. (2014). Patterns in the Galápagos magmatism arising from the upper mantle dynamics of plume-ridge interaction. In K. Harpp, E. Mittelstaedt, N. d'Ozouville, & D. Graham (Eds.), *The Galápagos: A Natural Laboratory for the Earth Sciences* (Vol. 1, pp. 245–261). Washington, DC: American Geophysical Union.

Ito, G., & Lin, J. (1995). Oceanic spreading center-hotspot interactions: Constraints from along-isochron bathymetric and gravity anomalies. *Geology*, *23*(7), 657–660. https://doi.org/10.1130/0091-7613(1995)023<0657:OSCHIC>2.3.CO;2

Ito, G., Lin, J., & Gable, C. (1997). Interaction of mantle plumes and migrating mid-ocean ridges: Implications for the Galápagos plume-ridge system. *Journal of Geophysical Research*, *102*(B7), 15,403–15,417. https://doi.org/10.1029/97JB01049

Jefferson, A., Ferrier, K., Perron, J., & Ramalho, R. (2014). Controls on the hydrological and topographic evolution of shield volcanoes and volcanic ocean islands. In K. Harpp, E. Mittelstaedt, N. d'Ozouville, & D. Graham (Eds.), *The Galápagos: A natural laboratory for the Earth sciences* (Vol. 1, pp. 185–213). Washington, DC: American Geophysical Union.

Karnauskas, K. B., Mittelstaedt, E., & Murtugudde, R. (2017). Paleoceanography of the eastern equatorial Pacific over the past 4 million years and the geological origins of the modern Galápagos upwelling. *Earth and Planetary Science Letters*, *460*, 22–28. https://doi.org/10.1016/j.epsl.2016.12.005

Kauahikaua, J., Hildenbrand, H., & Webring, M. (2000). Deep magmatic structures of Hawaiian volcanoes, imaged by three-dimensional gravity models. *Geology*, *28*(10), 883–886. https://doi.org/10.1130/0091-7613(2000)28<883:DMSOHV>2.0.CO;2

Kinoshita, W. T. (1965). A gravity survey of the island of Hawai'i. *Pacific Science*, *19*, 339–340. https://doi.org/10.1016/0377-0273(79)90022-2

Kokfelt, T., Lundstrom, C., Hoernle, K., Hauff, F., & Werner, R. (2005). Plume–ridge interaction studied at the Galápagos spreading center: Evidence from ^{226}Ra–^{230}Th–238U and ^{231}Pa–^{235}U isotopic disequilibria. *Earth and Planetary Science Letters*, *234*(1-2), 165–187. https://doi.org/10.1016/j.epsl.2005.02.031

Langmuir, C., Klein, E., & Plank, T. (1992). Petrological systematics of mid-ocean ridge basalts: Constraints on melt generation beneath ocean ridges. *Mantle Flow and Melt Generation at Mid-Ocean Ridges*, *71*. https://doi.org/10.1029/GM071p0183

Macdonald, G. A. (1965). Hawaiian calderas. *Pacific Science*, *19*(3), 320–334. http://hdl.handle.net/10125/10752

Mahr, J., Kurz, M., Harpp, K., Geist, D., Bercovici, H., Pimentel, R., et al. (2016). Rejuvenescent volcanism on San Cristóbal Island, Galápagos: A late "plumer". Abstract V35C-3119, presented at 2016 Fall Meeting, AGU, San Francisco, CA, 12-16 December.

McBirney, A., & Williams, H. (1969). Geology and petrology of the Galápagos Islands. *Geology and Petrology of the Galápagos Islands*, *118*. https://doi.org/10.1130/MEM118

McDougall, I., Embleton, B., & Stone, D. (1981). Origin and evolution of Lord Howe Island, Southwest Pacific Ocean. *Journal of the Geological Society of Australia*, *28*(1-2). https://doi.org/10.1080/001676181087291

Meschede, M., & Barckhausen, U. (2000). The plate tectonic evolution of the Cocos-Nazca spreading center. *Proceedings of the Ocean Drilling Program Scientific Results*, *170*, 1–10.

Mittal, T., & Richards, M. A. (2017). Plume-ridge interaction via melt channelization at Galápagos and other near-ridge hotspot provinces. *Geochemistry, Geophysics, Geosystems*, *18*, 1711–1738. https://doi.org/10.1002/2016GC006454

Mittelstaedt, E., Soule, A., Harpp, K., & Fornari, D. (2014). Variations in crustal thickness, plate rigidity and volcanic processes throughout the northern Galápagos volcanic province. In K. Harpp, E. Mittelstaedt, N. d'Ozouville, & D. Graham (Eds.), *The Galápagos: A Natural Laboratory for the Earth Sciences* (Vol. 1, pp. 263–284). Washington, DC: American Geophysical Union.

Mittelstaedt, E., Soule, S., Harpp, K., Fornari, D., McKee, C., Tivey, M., et al. (2012). Multiple expression of plume-ridge interaction in the Galápagos: Volcanic lineaments and ridge jumps. *Geochemistry, Geophysics, Geosystems*, *13*, Q05018. https://doi.org/10.1029/2012GC004093

Monro, D., & Rowland, S. (1996). Caldera morphology in the western Galápagos and implications for volcano eruptive behavior and mechanisms of caldera formation. *Journal of Volcanology and Geothermal Research*, *72*(1-2), 85–100. https://doi.org/10.1016/0377-0273(95)00076-3

Morgan, J. (1971). Convection plumes in the lower mantle. *Nature*, *230*, 42–43. https://doi.org/10.1038/230042a0

Morgan, W. J. (1978). Rodriguez, Darwin, Amsterdam, ..., A second type of Hotspot Island. *Journal of Geophysical Research*, *83*(B11), 5355. https://doi.org/10.1029/jb083ib11p05355

Nordlie, B. E. (1973). Morphology and Structure of the Western Galápagos Volcanoes and a model for their origin. *Geological Society of America Bulletin*, *84*(9), 2931. https://doi.org/10.1130/0016-7606(1973)842.0.co;2

Pimentel, R., Harpp, K., Geist, D., Mahr, J., Bercovici, H., Cleary, Z., and Cordova M. (2016). Are you there plume? It's me, San Cristóbal: Geochemical evolution of a Galápagos Island. Abstract V35C-3118, presented at 2016 Fall Meeting, AGU, San Francisco, CA, 12-16 December.

Poland, M. (2014). Contrasting volcanism in Hawai'i and the Galápagos. In K. S. Harpp et al. (Eds.), *The Galápagos: A Natural Laboratory for the Earth Sciences, Geophysical Monograph* (Vol. 204, pp. 5–26). Washington, DC: American Geophysical Union.

Ribe, N. M. (1996). The dynamics of plume-ridge interaction: 2. Off-ridge plumes. *Journal of Geophysical Research*, *101*, 16,195–16,204. https://doi.org/10.1029/96JB01187

Rowland, S., Munro, D., & Perez-Oviedo, V. (1994). Volcan Ecuador, Galápagos Islands: erosion as a possible mechanism for the generation of steep sided basaltic volcanoes. *Bulletin of Volcanology*, *56*(4), 271–283. https://doi.org/10.1007/BF00302080

Rubin, K., & Sinton, J. (2007). Inferences on mid-ocean ridge thermal and magmatic structure from MORB compositions. *Earth and Planetary Science Letters*, *260*(1-2), 257–276. https://doi.org/10.1016/j.epsl.2007.05.035

Ryland, S. L. (1971). A gravity and magnetic dtudy of the Galápagos Islands. (Ph.D. dissertation), University of Missouri–Columbia.

Schilling, J., Kingsley, R., & Devine, J. (1982). Galápagos hot spot spreading center system: 1. Spatial petrological and geochemical variations (83°W–101°W). *Journal of Geophysical Research*, *87*(12), 5593–5610. https://doi.org/10.1029/JB087iB07p05593

Schwartz, D. (2014). Volcanic, structural, and morphological history of Santa Cruz Island, Galápagos Archipelago. (Master's thesis), Moscow, University of Idaho.

Schwartz, D., Wanless, V., Berg, R., Jones, M., Fornari, D., Soule, S., et al. (2018). Petrogenesis of alkalic seamounts on the Galápagos platform. *Deep Sea Research Part II: Tropical Studies in Oceanography*, *150*, 170–180. https://doi.org/10.1016/j.dsr2.2017.09.019

Schwartz, D. M., Soule, S. A., Wanless, V. D., & Jones, M. R. (2018). Identification of erosional terraces on seamounts: Implications for interisland connectivity and subsidence in the Galápagos Archipelago. *Frontiers in Earth Science*, *6*(88). https://doi.org/10.3389/feart.2018.00088

Shorttle, O., Maclennan, J., & Jones, S. (2010). Control of the symmetry of the plume-ridge interaction by spreading ridge geometry. *Geochemistry, Geophysics, Geosystems*, *11*, Q0AC05. https://doi.org/10.1029/2009GC002986

Simkin, T., Shagam, R., Hargraves, R., Morgan, W., Van Houton, F., Burk, C., et al. (1973). Origin of some flat-topped volcanoes and guyots. *Geological Society of America*, *132*, 183–194.

Sinton, J., & Detrick, R. (1992). Mid-ocean ridge magma chambers. *Journal of Geophysical Research*, *97*(B1), 197–216. https://doi.org/10.1029/91JB02508

Small, C. (1995). Observation of ridge-hotspot interactions in the Southern Ocean. *Journal of Geophysical Research*, *100*, 17,931–17,946. https://doi.org/10.1029/95JB01377

Stock, M., Bagnardi, M., Neave, D., Maclennan, J., Bernard, B., Buisman, I., et al. (2018). Integrated petrological and geophysical constraints on magma system architecture in the western Galápagos Archipelago: Insights from Wolf volcano. *Geochemistry, Geophysics, Geosystems*, *19*, 4722–4743. https://doi.org/10.1029/2018GC007936

Strange, W. E., Machesky, L. F., & Woollard, G. P. (1965). A gravity survey of the island of Oahu, Hawaii. *Pacific Science*, *19*, 350–353.

Tepp, G., Ebinger, C., Ruiz, M., & Belachew, M. (2014). Imaging rapidly deforming ocean island volcanoes in the western Galápagos archipelago, Ecuador. *Journal of Geophysical Research: Solid Earth*, *119*, 442–463. https://doi.org/10.1002/2013JB010227

Vigouroux, N., Williams-Jones, G., Chadwick, W., Dennis, G., Andres, R., & Johnson, D. (2008). 4D gravity changes associated with the 2005 eruption of Sierra Negra. *Geophysics*, *73*(6), WA29–WA35. https://doi.org/10.1190/1.2987399

Villagomez, D., Toomey, D., Geist, D., Hooft, E., & Solomon, S. (2014). Mantle flow and multistage melting beneath the Galápagos hotspot revealed by seismic imaging. *Nature Geoscience*, *7*(2), 151–156. https://doi.org/10.1038/ngeo2062

Villagomez, D., Toomey, D., Hooft, E., & Solomon, S. (2007). Upper mantle structure beneath the Galápagos Archipelago from surface wave tomography. *Journal of Geophysical Research*, *112*, B07303. https://doi.org/10.1029/2006JB004672

Walker, G. (1990). Geology and volcanology of the Hawaiian Islands. *Pacific Science*, *44*(4), 315–347.

Weatherall, P., Marks, K., Jakobsson, M., Schmitt, T., Tani, S., Arndt, J., et al. (2015). A new digital bathymetric model of the world's oceans. *Earth and Space Science*, *2*, 331–345. https://doi.org/10.1002/2015EA000107

Wilson, D., & Hey, R. (1995). History of rift propagation and magnetization intensity for the Cocos-Nazca spreading center. *Journal of Geophysical Research*, *100*(B6), 10,041–10,056. https://doi.org/10.1029/95JB00762

Wilson, E. (2013). The geochemical evolution of Santa Cruz Island, Galápagos Archipelago, (Masters Thesis). Moscow, University of Idaho.